DAMAGE KINETICS IN FERRITIC SPHEROIDAL GRAPHITE CAST IRON

C. Guillemer-Neel*, X. Feaugas*, V. Bobet†, M. Clavel*

This study mainly focuses on the damage processes in nodular cast iron. Void nucleation and growth evolutions are described as functions of mechanical parameters ($\underline{\underline{\Sigma}}$, $\underline{\underline{\varepsilon}}$). Damage kinetics are compared with previous models. It is shown that nucleation law corresponds to Needleman and Rice model (1) and the growth law fits the Gurson-Tvergaard one (Tvergaard (2)). Finally a critical damage volume fraction f^c is obtained. It is found that f^c depends on the triaxiality rate.

INTRODUCTION

Numerous damage studies have been carried out in alloys containing hard inclusions. It has been established that for particles which dimension is greater than 1 μm, the nucleation of cavity requires the attainment of a critical interfacial stress (Argon (3) Beremin (4)). More recent studies reported the influence of others metallurgical parameters on nucleation process, such as the local volume fraction expressed by the d/2R ratio where d represents the half distance between inclusions and R the radius of the inclusion ((3), Guillemer *et al.* (5)). Improvement in the theoretical approach (Gilormini (6)) to account for the effect of triaxiality, plastic strain and porosity necessitates extensive experimental research on void nucleation and growth kinetics. The aim of the present study is also to determine damage kinetics in nodular cast iron from an experimental approach. Then these kinetics are compared with previous models ((1), (2)).

* Université de Technologie de Compiègne, LG2MS URA 1505, Compiègne, BP529.
† Renault, Direction de la recherche, Sce 60152, Boulogne-Billancourt cedex, F-92109.

MATERIAL AND EXPERIMENTAL PROCEDURE

The nodular cast iron is composed of graphitic nodules surrounded by a Fe3%Si matrix (with less than 5% of perlite). The volume fraction of inclusions f_0 is about 13 pct, the mean ferritic grain size and the mean diameter of nodules are ϕ_α = 21 µm and 2R = 16 µm respectively. Using Dirichlet tessellation technique, the spatial distribution of the particles (d/2R ratio) was determined on an area of 1.4 mm^2 which corresponds to 750 particles (figure 1).
The evolution of the damage was studied in the frame of the local approach of fracture. This method has been largely described elsewhere ((3), (4), Helbert *et al.* (7)). The use of axisymetric smooth and notched specimens allows to examine large ranges of stress triaxiality (χ) and equivalent plastic strain (ε_{peq}).
A finite element calculation was performed for each specimen design to provide the mechanical parameters distribution in the bulk of the specimen during loading. The plastic law was determined from tensile tests results and numerically identified in the framework of the classical elastoplastic theory without damage, based on the thermodynamics of irreversible processes with internal variables (7). The validity of such finite element modeling (FEM) calculations was checked by comparing the numerical loading curves with the experimental ones up to necking and fracture.
To quantify damage, specimens were tested to fracture or interrupted before fracture, longitudinally cut and mechanically polished. An ion milling technique was used after polishing to avoid the artefact linked to grinding or polishing. Nucleation and growth of damage were examined in a scanning electron microscope (SEM) on surface elements representative of the microstructure. For each element, the mechanical parameters do not vary more than 10 pct.

EXPERIMENTAL RESULTS AND DISCUSSION

Void nucleation kinetics: because of strain incompatibilities between the inclusion and the matrix, the stress components evolve in the vicinity of the particle. The interfacial stress is expressed as the sum of two components: the stress in the matrix and an additional stress resulting from the heterogeneity of plastic deformation. Following this way the interfacial stress is written as a function of two macroscopic stresses: the hydrostatic stress (Σ_m) and an internal stress induced by strain incompatibilities ($B\varepsilon_{peq}$ where ε_{peq} represents the equivalent Von Mises plastic strain) (3, 4). The inclusion/matrix interface fails for a critical value of this function:

$$\sigma_i^c = A\,\Sigma_m + B\,\varepsilon_{peq} \quad \text{..... (1)}$$

Such an approach no longer applies to the nodular cast iron in which the volume fraction of inclusions is important enough to generate continuous nucleation (5). Previous FEM calculations conducted on hard particle surrounded by an homogeneous matrix have evidenced interaction effects between closely spaced inclusions (5): the interfacial stress increases as the d/2R ratio decreases and the interaction effect progressively vanishes for ratios greater than .3. The figure 2 shows the critical couples (Σ_m, ε_{peq}) associated with a cumulated percentage of damaged nodules in terms of decohesion ($\%DN_c$). In the experimental ranges of mechanical parameters a linear relationship between Σ_m and ε_{peq} is obtained, *i.e.*:

$$\Sigma_c = f(\Sigma_m, \varepsilon_{peq}) = \Sigma_m + 6130\,\varepsilon_{peq} \quad \text{..... (2)}$$

in which Σ_c evolves as a function of the percentage of damage nucleation:

$$\Sigma_c = g(\%DN_c) = 5.1\,(\%DN_c) + 370 \quad \text{..... (3)}$$

FEM results show that the closest inclusions nucleate cavities first. To describe nucleation kinetics, both figure 1 and relation (3) are used. When Σ_c equals 500 MPa for instance, 25 pct of nodules have initiated voids. These particles exhibit a d/2R ratio lower than 0.4. Following this process, a category of damaging d/2R (figure 3) and an instantaneous percentage of damaging inclusions :$\%DN_i$ (figure 4) can be associated with an increment of Σ_c. The figure 3 suggests that interaction effect no longer intervenes for d/2R ratios greater than 0.3 since Σ_c tends to saturate when the ratio equals 1.2. A such ratio corresponds to a distance between inclusions $2d = 2\phi_\alpha$. This gap between calculations and experimental results could be related to the anisotropy of the medium between inclusions.
Void nucleation kinetics, as it is shown in the figure 4, can be represented by a normal distribution: $\%DN_i = A \exp\left[-\frac{1}{2}\left(\frac{\Sigma_c - \Sigma_{cmean}}{s_n}\right)^2\right] = A\,\mathcal{G}(\Sigma_c)$ ..... (4)
where the pre-exponential factor A = 0.1, the mean void nucleation stress $\Sigma_{c\ mean}$ = 580 MPa and the standard deviation s_n = 145 MPa are experimentally determined.
The evolution of void volume fraction is given by $df_N = C\ \mathcal{G}(\Sigma_c)\ d\Sigma_c$..... (5)
with $C = 3.8\ 10^{-4}$. It is worth emphasizing that the previous relation is similar to the Needleman-Rice law for continuous nucleation (1). From the relation (4), nucleation kinetics *vs* Σ_m or ε_{peq} can be deduced as well as the dependence of kinetics on the microstructure (d/2R distribution).

Void growth kinetics: the elliptic growth of cavities has been studied in a S.E.M. in representative surface elements and characterized by Image Analysis (see figure 5). The minor axis (a) remains constant and equal to the initial diameter of the particle whatever the plastic strain or the triaxiality factor as it was previously checked (Guillemer *et al.* (8)). On each surface element, the ratio b/a follows a normal distribution. Since the growth rate is assumed to be independent on geometrical parameters (d/2R, initial cavity size, etc.), the evolution of either the mean ratio d/2R or the maximum one can be examined as a function of χ and ε_{peq}. Growth kinetics at various triaxialities are given in the figure 5 and are expressed by the following relation: $b/a = V \exp(U\varepsilon_{peq})$..... (6)
The parameters U et V are identified for each triaxiality in order to fit the experimental results at best (figures 5 and 6).
Numerous studies have provided analytical laws to describe a single-void growth (6) and generally agree with the classical growth law: $dR/R = f(\chi)\ d\varepsilon_{peq}$ where R is the mean void radius. Among these analyses, the Gurson-Tvergaard model seems to be more appropriate to describe void growth since it takes into account a randomly distributed volume fraction of voids f (2). Gurson's yield function is written as follows: $\phi = J2(\underline{\underline{\Sigma}} - \underline{\underline{X}}) - (R + k)\,[1 + f^2 - 2f\,q_1 \cosh(3/2\,q_2\,\chi)]^{1/2}$ ..... (7)
where q_1 and q_2 were introduced by Tvergaard (q_1 = 1.5, q_2 =1). Assuming macroscopic normality rule, the hydrostatic strain rate $d\varepsilon_{kk}$ is obtained: $d\varepsilon_{kk} = d\varepsilon_{peq}\ d\phi/d\Sigma_m$. Moreover $d\varepsilon_{kk} = f\,dV_{void}/V_{void} = f\,db/b$. From these equations and neglecting the second order terms in the Gurson's potential, the void growth law according to Gurson-Tvergaard can be deduced. Comparing this one with the previously introduced one (equation 6), U is obtained as a function of q_1 and q_2:
$U = 3/2\ q_1 q_2 \sinh(3/2\ q_2\ \chi)\ d\varepsilon_{peq}$..... (8)
From experimental results on void growth kinetics, the constants q_1 and q_2 are evaluated: q_1 = 1.85 and q_2 =1.07 (see figure 6). The high value of q_1 results from interactions between neighboring inclusions which enhance the growth process

((6), Marini *et al.* (9)). Assuming the plastic incompressibility of the matrix, it comes: $df_G = (1 - f)\, d\varepsilon_{kk}$ where f_G represents the growth volume fraction.

Critical damage volume fraction: using the mechanical parameters at fracture (as it is shown in the figure 2b), the critical volume fraction of voids associated with the nucleation process (f_N^c) and the one associated with the growth event (f_G^c) can be determined. It is observed that the void nucleation process is a predominant damage factor whatever the triaxiality rate. The total damage volume fraction at fracture ($f^c = f_N^c + f_G^c$) is reported as a function of χ on the figure 7. It is worth emphasizing that the critical fraction represents no material characteristic. Indeed, on the contrary to previous results obtained for titanium alloys (7), f^c increases when the triaxiality rate decreases. Evolution of f^c for various volume fractions of inclusions (f_0) are added on the figure 7 ((7), Zhang and Niemy (10)). In any case, a linear relationship is obtained between f^c and χ. The slope p of the curve $f^c = g(\chi)$ increases with the initial volume fraction of inclusions, following: $|p| = 1.114\ f_0$. This dependence can probably be explained by the difference in the void coalescence processes according to the triaxiality.

CONCLUSION

Void nucleation and growth kinetics have been experimentally determined for ferritic nodular cast iron. These two processes are increasing functions of plastic strain and triaxiality rate. The continuous nucleation is explained in terms of interaction between closely spaced inclusions. The experimentally determined damage kinetics are compared to theoretical models ((1), (2)). Such an comparison allows to identify the parameters q_1 and q_2 introduced in the Gurson's potential. The determined values are similar to the ones proposed by Tvergaard. Finally the critical damage volume fractions (f^c, f_N^c, f_G^c) are evaluated and it is observed that f^c evolves with the triaxiality. It is worth emphasizing that the high volume fraction is an important factor in the nodular cast iron since it results in interaction effects in the whole process of ductile fracture. However rather than the global volume fraction, the local volume fraction (d/2R) is the very essential parameter.

REFERENCES

(1) A. Needleman, J.R. Rice, in DP. Koitinen and NM. Wang (eds), Mechanics of Sheet Metal Forming, Plenum, 237 (1978)
(2) V. Tvergaard, Int. J. of Fract., 17, 389 (1981)
(3) A.S. Argon, J. Im, Met. Trans., 6A, 839 (1975)
(4) F. M. Beremin, Met. Trans., 12A, 723 (1981)
(5) C. Guillemer-Neel, A.S. Béranger, M. Clavel, Proceedings of the 11th ECF, 843 (1996)
(6) P. Gilormini, C. Licht, P. Suquet, Arch. Mech., 40, 43 (1988)
(7) A.L. Helbert, X. Feaugas, M. Clavel, Acta Met., 46, 939 (1998)
(8) C. Guillemer-Neel, X. Feaugas, V. Bobet, M. Clavel, Proceedings of the National Conference Mecamat, 43 (1998)
(9) B. Marini, F. Mudry, A. Pineau, Eng. Fract. Mech., 22, 989 (1985)
(10) Z. L. Zhang, E. Niemy, Int. J. of Fract., 70, 321 (1995)

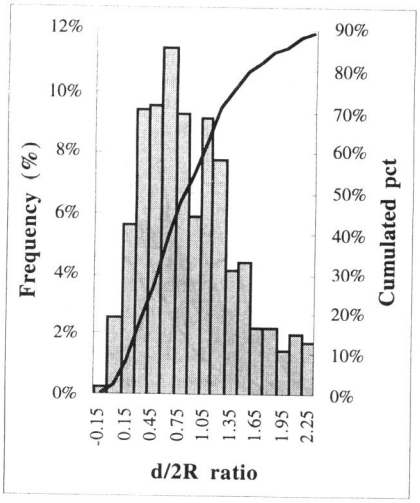

Figure 1: Dirichlet tessellation results distribution of the d/2R ratio

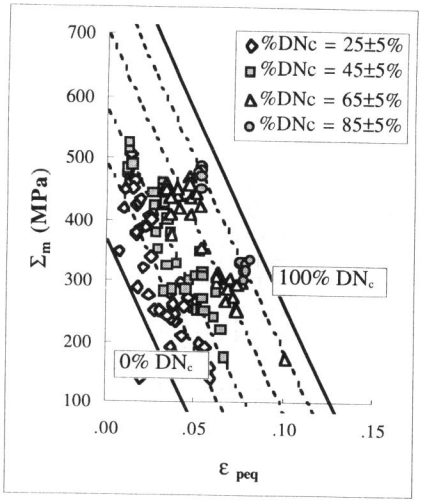

Figure 2a: Critical couples (Σ_m, ε_{peq}) associated with a pct of nucleation $(\%DN)_c$

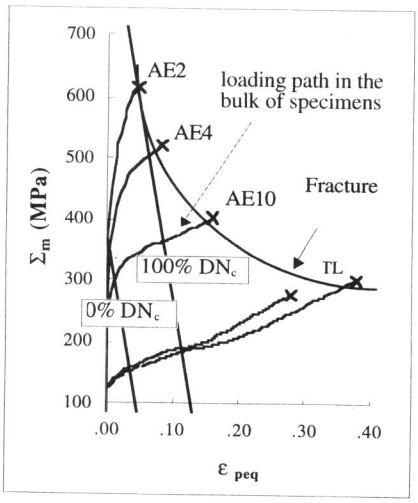

Figure 2b: loading path and damage in the specimens

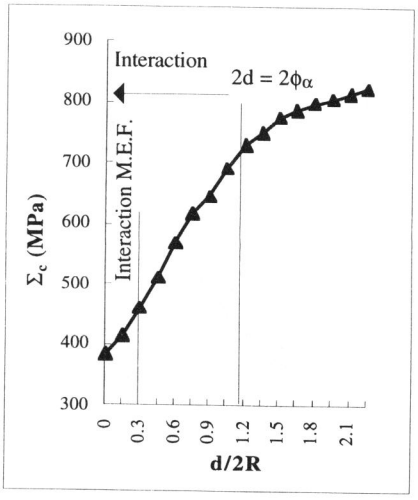

Figure 3: Evolution of Σ_c versus d/2R

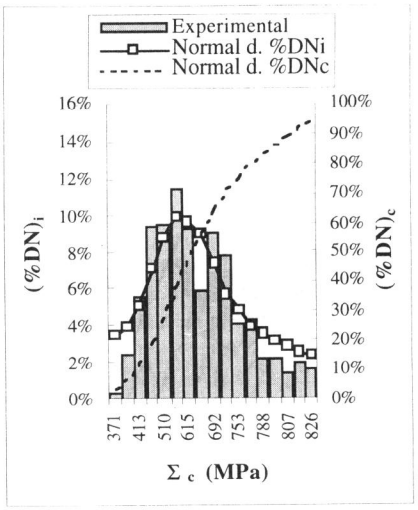

Figure 4: Nucleation kinetics versus Σc Experimental and Normal distributions

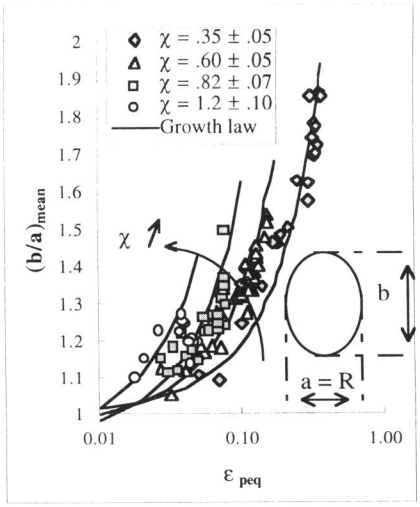

Figure 5: Growth kinetics $(b/a)_{mean}$ at various triaxialities

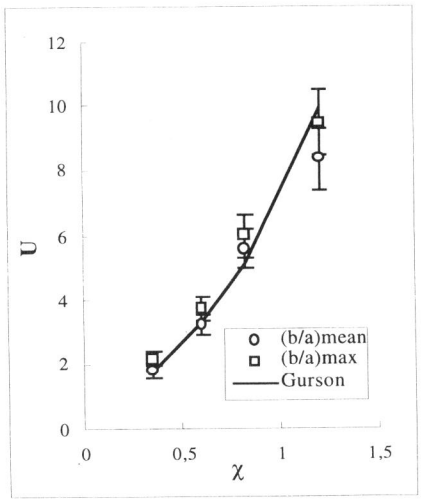

Figure 6: Evolution of U (kinetics) Experimental and Gurson-Tvergaard law

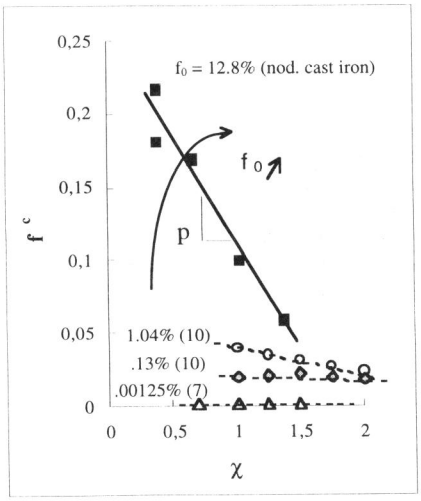

Figure 7: Critical damage fraction as a function of χ and f_0